IMPROVED LUMPED PARAMETER MODEL FOR PHASE CHANGE IN LATENT THERMAL ENERGY STORAGE SYSTEMS

Mina Rouhani, Majid Bahrami
Laboratory for Alternative Energy Conversion (LAEC),
School of Mechatronic Systems Engineering, Simon Fraser University, V3T 0A3
+1 (778) 782-8538/ mbahrami@sfu.ca

Abstract

A modified lumped parameter model has been used to study transient conduction in phase change materials (PCM) in cylindrical coordinates. The two-point Hermite approximation is used to compute the average temperatures and the temperature gradient in each phase. The performance of PCM has been analyzed during the charging processin terms of energy storage and density. The effect of Stefan number on melting front dynamics is comprehensively studied. The results are verified with exact solutions as well as steady-state asymptotes and also show good agreement with existing experimental data.

KEYWORDS

Stefan problem; Lumped model; phase change material (PCM); Thermal energy storage; Solidification;Hermite approximation

INTRODUCTION

Thermal energy storage (TES) systems are a sustainable, energy efficient alternative to conventional heating and cooling methods. TES can play a pivotal role in synchronizing energy demand and supply, both on a short and long term basis.TES is divided into sensible, latent, and thermochemical mechanisms. Latent thermal storage using phase change materials(PCM) has a relatively constant melting/solidification temperature,higher energy storage density compared to sensible TES,and less complexity and lower manufacturing cost than the thermochemical TES [1].

Due to the non-linearity of phase change problems, analytical solutions to the analysis of phase change problem are limited by assumptions such as small Stefan number, specific boundary conditions, and simple geometries. The Stefan number,*Ste*, represents the ratio of the sensible heat to the latent heat. The assumption of small Stefan number limits such models to materials and operating temperature conditionswhere the sensible heat is much smaller than the latent heat. Stefan's early study of the solidification front solution assumed the liquid is maintained at the melting temperature, simplifying the model to a single phase problem [2]. Neumann [3]developed a two-phase solution for asemi-infinite region at constant temperature greaterthan the temperature of fusion with the solid-liquidinterface at the temperature of fusion.Paterson [4]developed a simple exact solution incylindrical coordinates with supply or removal of heat by a continuous line source. For regions bounded internally or externally by a circular cylinder with constant surface temperature, the geometry considered in this paper, there are no analytical solutions available in the literature to the best of our knowledge.Moreover, there are no closed form solutions for the problem with volumetric heat generation or other boundary conditions such as constant heat flux or radiation.

Phase change problems with complex geometry, turbulent flow, temperature dependent properties, liquid motion, radiation flux, and material with internal heat source or sink, are usually solved by using numerical methods [5,6]. Numerical solutions for phase change problems come in two classes: front-tracking methods and fixed-grid enthalpy methods[7]. In general, the front-tracking methods are accuratebut limited to simple geometries ascomplex geometries require massive parallel computing on a moving mesh. Sharp tracking

techniques are required to accurately capture the dynamics of the interface [8]. In a new front tracking method, Lattice-Boltzmann simulation is applied to treat the latent-heat source term by modifying the equilibrium distribution function for the temperature[9]. The fixed-grid approach is simpler and more practical. In this method, latent heat is usually absorbed into the enthalpyof the system, which is treated as a temperature dependent variable,and latent heat flow is constructed through volume integration [10].

Approximation methods can also be applied to solve Stefan problem. Goodman [11] developed an integral equation thatexpresses the overall heat balance of the system by integrating the one-dimensional heat conduction equation with respect to the spatial variable and inserting boundary conditions. In this method, selecting a proper approximation ofthe temperature distribution is difficult; the use of a high-order polynomial complicates this approachand maynot improve the accuracy of the solution.Mitchell and Myers [12] have developed a combined integral method by combining the standard integral and refined integral methodsproposed by Sadoun and Si-Ahmed [13,14]. A quasi-steady approximation was applied byJiji and Gaye [15]to study one-dimensional solidification and melting of a slab with uniform volumetric heat generation.In this common approximation, it is assumed that the transient term in the heat equation can be neglected for small *Ste*.

Considering the complexity and cost of numerical solutions as well as the limiting assumptions made in the existing analytical and approximation methods, there is a need for a more general and easy-to-use solution that can predict the effects of important parameters on solidification and melting.Semi-analytical solutions are an alternative method to deal with the complexity of the phase-change problems. Mirzaei*et al.*[16] proposed a one-dimensional semi-analytical lumped model using a resistance-capacitance (RC) circuit concept containing variable capacities, where the nonlinear energy balance equations were solved by numerical approach [16]. The lumped parameter method is a practical solution for solving heat conduction problems, although it has a restriction for Biot number (i.e.,$Bi<0.1$). Asthe heat conduction coefficient in PCM is low, the classical lumped method is not well fitted to the phase change problem.Cotta and Mikhailov [17] proposed an improved lumped parameter method for steady and transient heat conduction problems based on Hermite approximation for integrals that define averaged temperature and heat fluxes.An and Su [18] used this improved method for the melting process in a slab.

In the present study, an improved lumped parameter model is used to examine the phase change process using the Hermite two-point approximation in cylindrical coordinates. Unlike previous analytical models,this model has no limitation for *Ste*, temperature, or boundary conditions, and can be easily implemented for phase change processes.The goal of this study is to develop a general easy-to-use method thatcaptures the phase change process in cylindrical coordinates, which are widely used in the energy industry.

MODEL DEVELOPMENT

In the present work, the one-dimensional transient melting process in an annular pipe is considered. The two walls are maintained at a constant temperature and the temperature at the solid-liquid interface, $S(t)$, isT_m, the melting temperature.The schematic of the problem in cylindrical coordinates is shown in Fig. 1.The volumetric heat generation,$\dot{q}$, is considered in this model. Initially, the PCM is at a temperature lower than the melting temperature. Afterwards, the innerwall temperature increases toT_b,i.e., higher than the melting temperature, and the melting front starts moving.The following assumptions are employed to the analysis of the melting process in PCMs: (1) the physical properties of both phases are constant; (2) the mushy melting front is assumed to be a line; (3) melting occurs at a constant temperature,T_m; (4) motion of liquid phase is negligible; (5) whenever heat generation rate is considered throughout the solid and liquid regions, it is assumed to be uniform and time-independent; (6) the changes in volume during phase change are negligible.

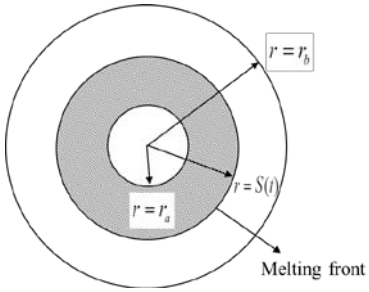

Fig. 1. The schematic of melting in annular pipes

Using the above assumptions, heat conduction equations in liquid and solid can be written as follows:

$$\frac{\partial T_i(r,t)}{\partial t} = \alpha_i \frac{1}{r}\frac{\partial}{\partial r}\left(r^{n-1}\frac{\partial T_i(r,t)}{\partial r}\right) + \frac{\dot{q}_{gen}}{\rho_i c_{p,i}}, \qquad i = l, s \qquad 1)$$

where *l* and *s* represent properties of liquid and solid phase, respectively.The energy balance at the interface of solid and liquid phasesis:

$$k_l \frac{\partial T_l(r,t)}{\partial r} + \rho_s L \frac{\partial S(t)}{\partial t} = k_s \frac{\partial T_s(r,t)}{\partial r}, \qquad (2)$$

The governing equations, boundary conditions, and initial conditions in dimensionless form are given in Table 1.

Table 1. Dimensionless governing equations, boundary conditions, and initial conditions

$\frac{\partial \theta_l}{\partial Fo} = \alpha^* \frac{1}{\xi}\frac{\partial}{\partial \xi}\left(\xi \frac{\partial \theta_l}{\partial \xi}\right) + \frac{\alpha^* q^*_{gen}}{k^*}$, $\varepsilon < \xi < \eta(Fo)$	$\frac{\partial \theta_s}{\partial Fo} = \frac{1}{\xi}\frac{\partial}{\partial \xi}\left(\xi \frac{\partial \theta_s}{\partial \xi}\right) + q^*_{gen}$, $\eta(Fo) < \xi < 1$
$k^* \frac{\partial \theta_l}{\partial \xi} + \frac{1}{Ste}\frac{\partial \eta(Fo)}{\partial Fo} = k_s \frac{\partial \theta_s}{\partial \xi}$, $\xi = \eta(Fo)$	$\theta_l(\eta(Fo), Fo) = \theta_s(\eta(Fo), Fo) = 1$
$\theta_l(\varepsilon, Fo) = \theta_a$ $\quad \theta_s(\xi, 0) = \theta_i$	$\theta_s(1, Fo) = \theta_b$ $\quad \eta(0) = \varepsilon$

The dependence of the interface velocity on the temperature gradient causes the phase change conduction equations to be non-linear. There are exact solutions for one-dimensional phase change in a semi-infinite region and small *Ste*. Therefore, approximate, numerical, or semi-analytical solutions should be usedfor analyzing the phase change process in a confined region[3].The present semi-analytical model is an improved lumped model using Hermite approximation. In the present lumped parameter model, the spatially averaged dimensionless temperature of the liquid and the solid are defined as follows

$$\bar{\theta}_l(Fo) = \frac{2}{\eta^2(Fo) - \varepsilon^2}\int_{\varepsilon}^{\eta(Fo)} \xi \theta_l(\xi, Fo) d\xi \qquad \varepsilon < \xi < \eta(Fo) \qquad (3)$$

$$\bar{\theta}_s(Fo) = \frac{2}{1 - \eta^2(Fo)}\int_{\eta(Fo)}^{1} \xi \theta_s(\xi, Fo) d\xi \qquad \eta(Fo) < \xi < 1 \qquad (4)$$

Spatial integrating of theenergy equations of each phase,and considering the averaged temperatures defined in Eqs. (3) and (4), the following are obtained

$$\frac{d}{dFo}\left(\bar{\theta}_l\left(\eta^2(Fo) - \varepsilon^2\right)\right) - 2\left(\xi\theta_l\right)\Big|_{\xi=\eta(Fo)}\frac{d\eta(Fo)}{dFo} = 2\alpha^*\left(\xi\frac{\partial \theta_l}{\partial \xi}\right)\Big|_{\xi=\varepsilon}^{\xi=\eta(Fo)} + \frac{\alpha^* q^*_{gen}}{k^*}\left(\eta^2(Fo) - \varepsilon^2\right), \qquad 5)$$

$$\frac{d}{dFo}\left(\bar{\theta}_s\left(1-\eta^2\left(Fo\right)\right)\right)-2(\xi\theta_s)\big|_{\xi=\eta(Fo)}\frac{d\eta(Fo)}{dFo}=2\left(\xi\frac{\partial\theta_s}{\partial\xi}\right)\Bigg|_{\xi=\eta(Fo)}^{\xi=1}+q^*_{gen}\left(1-\eta^2\left(Fo\right)\right), \quad 6)$$

In an attempt to improve the approximation approach of the classical lumped model, some work has been done based on Hermite-type approximations for integrals [19,20]. In the present work, lumped transient heat conduction with melting in an annular pipe is solved using Hermite-type approximation. Using the general Hermite approximation makes it possible to write an integral of a function as a combination of the function and its derivatives at the integration limits in the following form[21]

$$H(\alpha,\beta)=\int_a^b z(y)\,dy=\sum_{v=0}^{\alpha}C_v(\alpha,\beta)\,h^{v+1}\,z^{(v)}(a)+\sum_{v=0}^{\beta}C_v(\beta,\alpha)(-1)^v h^{v+1}z^{(v)}(b)+O(h^{\alpha+\beta+3}) \quad 7)$$

where$C_v(\alpha,\beta)=((\alpha+1)!(\alpha+\beta+1-v)!)/((v+1)!(\alpha-v)!(\alpha+\beta+2)!)$,and$h=b-a$. In the lumped model, a relation between boundary temperatures, averaged temperatures, and temperature gradient at two walls and the liquid-solid interface is achievable by implementing the Hermite-type approximation. In the present model,*H(0,0)* is used for the product of length and temperature gradients, and*H(1,1)* is used for averaged temperatures, as follows:

$$\int_{\varepsilon}^{\eta(Fo)}\frac{\partial(\xi\theta_l)}{\partial\xi}d\xi=(\xi\theta_l)\big|_{\eta(Fo)}-(\xi\theta_l)\big|_{\varepsilon}\cong\frac{\eta(Fo)-\varepsilon}{2}\left[\frac{\partial(\xi\theta_l)}{\partial\xi}\bigg|_{\varepsilon}+\frac{\partial(\xi\theta_l)}{\partial\xi}\bigg|_{\eta(Fo)}\right] \quad 8)$$

$$\int_{\eta(Fo)}^{1}\frac{\partial(\xi\theta_s)}{\partial\xi}d\xi=(\xi\theta_s)\big|_{1}-(\xi\theta_s)\big|_{\eta(Fo)}\cong\frac{1-\eta(Fo)}{2}\left[\frac{\partial(\xi\theta_s)}{\partial\xi}\bigg|_{1}+\frac{\partial(\xi\theta_s)}{\partial\xi}\bigg|_{\eta(Fo)}\right] \quad 9)$$

$$\bar{\theta}_l\cong\frac{\eta\left(Fo\right)-\varepsilon}{\eta^2\left(Fo\right)-\varepsilon^2}\left((\xi\theta_l)\big|_{\varepsilon}+(\xi\theta_l)\big|_{\eta(Fo)}\right)+\frac{\left(\eta\left(Fo\right)-\varepsilon\right)^2}{6\left(\eta^2\left(Fo\right)-\varepsilon^2\right)}\left[\frac{\partial(\xi\theta_l)}{\partial\xi}\bigg|_{\varepsilon}-\frac{\partial(\xi\theta_l)}{\partial\xi}\bigg|_{\eta(Fo)}\right] \quad 10)$$

$$\bar{\theta}_s\cong\frac{1-\eta\left(Fo\right)}{1-\eta^2\left(Fo\right)}\left((\xi\theta_s)\big|_{\eta(Fo)}+(\xi\theta_s)\big|_{1}\right)+\frac{\left(1-\eta\left(Fo\right)\right)^2}{6\left(1-\eta^2\left(Fo\right)\right)}\left[\frac{\partial(\xi\theta_s)}{\partial\xi}\bigg|_{\eta(Fo)}-\frac{\partial(\xi\theta_s)}{\partial\xi}\bigg|_{1}\right] \quad 11)$$

The system of equations formed by Eqs. (5), (6), (8)-(11), and the interface energy balance can be solved analytically. After implementing the constant wall temperatures in these equations, a system of three ordinary differential equations for the location of interface, averaged temperatures of liquid and solidis obtained as follows:

$$\frac{d\eta(Fo)}{dFo}=Ste\left[\frac{-3\eta(Fo)-(2\theta_b+1)+3\bar{\theta}_s\left(1+\eta\left(Fo\right)\right)}{\eta\left(Fo\right)\left(1-\eta\left(Fo\right)\right)}-k^*\frac{3\eta(Fo)+\varepsilon(2\theta_a+1)-3\bar{\theta}_l\left(\varepsilon+\eta\left(Fo\right)\right)}{\eta\left(Fo\right)\left(\eta\left(Fo\right)-\varepsilon\right)}\right] \quad 12)$$

$$\frac{d\bar{\theta}_l(Fo)}{dFo}=\frac{2(1-\bar{\theta}_l)}{\left(\eta^2\left(Fo\right)-\varepsilon^2\right)}\eta\left(Fo\right)\frac{d\eta\left(Fo\right)}{dFo}+\frac{2\alpha^*}{\left(\eta^2\left(Fo\right)-\varepsilon^2\right)}\left(\frac{\eta\left(Fo\right)(5+\theta_a)+\varepsilon\left(5\theta_a+1\right)-6\bar{\theta}_l\left(\eta\left(Fo\right)+\varepsilon\right)}{\eta(Fo)-\varepsilon}\right)+\frac{\alpha^*q}{k} \quad 13)$$

$$\frac{d\bar{\theta}_s(Fo)}{dFo}=\frac{2(1-\bar{\theta}_s)}{\left(1-\eta^2\left(Fo\right)\right)}\eta(\mathrm{Fo})\frac{d\eta\left(Fo\right)}{dFo}+\frac{2}{\left(1-\eta^2\left(Fo\right)\right)}\left(\frac{\eta\left(Fo\right)(5+\theta_b)+\left(5\theta_b+1\right)-6\bar{\theta}_s\left(1+\eta\left(Fo\right)\right)}{1-\eta(Fo)}\right)+q^*_{gen} \quad 14)$$

The above system of equations was solved usinga stiff MATLAB ordinary differential equation (ODE)solver by assuming that initially the melting front was at the inner radius and both phases were at the same initial temperature.

RESULTS

Melting of phase change materials in cylindrical coordinate is analyzed byimproved lumped-parameter model with Hermite approximation. For verification,the proposed model is comparedagainstavailable asymptotic analyticalsteady-state solution as well as experimental data.

Case I. Solidification due to a line heat sink atthe center of a cylindrical pipe

In this section, solidification in a cylinder with a central heat sink is studied. The present model is applied to this problem and the results are compared to the asymptotic solutions for long and short terms.A line heat sink ($\lim_{\xi\to 0}(\xi\partial\theta_s/\partial\xi)=Q/(2\pi k_s(T_m-T_b))=Q^*$)is placed in the center of the cylinder,while at outer radius constant temperature$\theta_b$is imposed. For the short time solution, when solidification penetration is much smaller than the radius of the cylinder, the phase change problem is equivalent to solidification by a line heat sink in an infinite medium with cylindrical symmetry. Paterson [4]reported the exact solution for this problem using an exponential integral function in the form of$Ei(-r^2/4\alpha t)$. Consequently, the dimensionless interface energybalance is as follows,

$$\frac{Q^*}{2}\exp(-\lambda)+k^*(\mathrm{T}_i-\mathrm{T}_m)\Big/\Big(\big(T_m-T_{ref}\big)Ei\big(-\lambda/\alpha^*\big)\Big)=\frac{\lambda}{Ste} \tag{15}$$

where solidification interface can be obtained from$\eta(Fo) = (4\lambda\tau)^{1/2}$. For the long-term asymptote,the steady state solution is considered by setting the derivative of temperature with respect to time equal to zero.Figure2 shows the comparison of the present model with short and long-term asymptotes. In small Fourier numbers (early moments of solidification), the model well matches the short-term asymptote while for high Fo numbers, it is fitted to the steady-state solution asymptote.

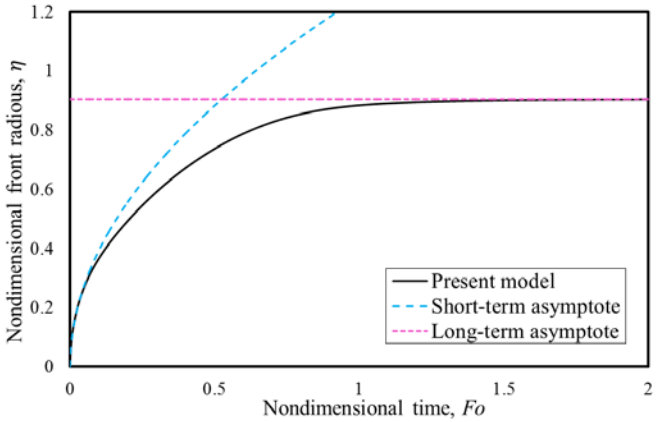

Fig. 2. Comparison between solidification frontsfromthe present model,the short term, and long term asymptotes

Case II.Solidification in annular pipes with constant temperature at walls

The model results were compared to the experimental study of Sparrow [22] in whicha test cell wassituated in a temperature-controlled water bath to maintain a constant outer wall temperature.Figure 3 (a) depicts a schematic of the experimental apparatus used in [22]. The phase change medium was paraffin, 99% pure n-eicosane, with a melting temperature of 36.4°C.The inner and outer walls werekept at constant temperatures of 8.6˚Cand 54.2˚C, respectively.The interface location was read to 0.01 mm (Vernier caliper) and thermocouple outputs were monitored by a voltmeter (± 0.1μV).The properties of paraffin wax (n-eicosane),listed in Table 2,were used in the model.The thermal conductivity valueswere measured via steady-state method [23] and by transient plane source (TPS) [24]. In latter study, the effect of three different methods of solidification on solid thermal conductivity was assessed; ambient solidification, ice-water bath solidification, and oven solidification.In all methods, thermal conductivity of n-eicosanevaried little from10 to 33˚C, and

sharply rose at temperatures from 33 to 35°C because of the non-equilibrium state of n-eicosane near phase transition. Moreover, thermal conductivity obtained from the ambient solidification method was close to the experimental data in Ref. [23]. It was reported that in ice-water bath solidification, a fast process, the rapidly formed solid paraffin was porous which led to lower thermal conductivity compared to denser paraffin formed by slowersolidification methods.In the present study, the solid thermal conductivity at the minimum and maximum reported temperatures and ambient solidification methodare consideredin order to check the validity of the model and sensitivity of the results to the solid thermal conductivity.

Table 2. Physical properties of n-eicosane

Properties	**Solid**	**Liquid**
Melting Point*(°C)*	36.4 [25]	-
Heat of fusion*(kJ/kg)*	247.3[25]	-
Density*(kg/m^3)*	778[25]	856[25]
Thermal conductivity*(W/(mK))*	0.42[23] , 0.4212-0.5503 [24]	0.150[25]
Specific heat*(kJ/(kgK))*	2.010[25]	2.210[25]

Figure 3 (b)shows the comparison between Sparrow's experimental data [22] and the results obtained from the present model fork_s=0.4212 andk_s=0.5503, which are the reported solid thermal conductivity at 10°Cand 35°C in ref. [24]. The present model shows good agreementwith the experimental data.The maximum relative difference between the experimental data and the present results, which is fork_s=0.4212, is approximately 9.5%; this discrepency is due to the uncertainty of the experiment, the nature of whisker-like crystals at the interface, and the accuracy of the solid thermal conductivity.We noticed that the model's results are very sensitive to the solid thermal conductivity. The maximum relative difference between the results fork_s=0.4212and k_s=0.5503is 7.7%.

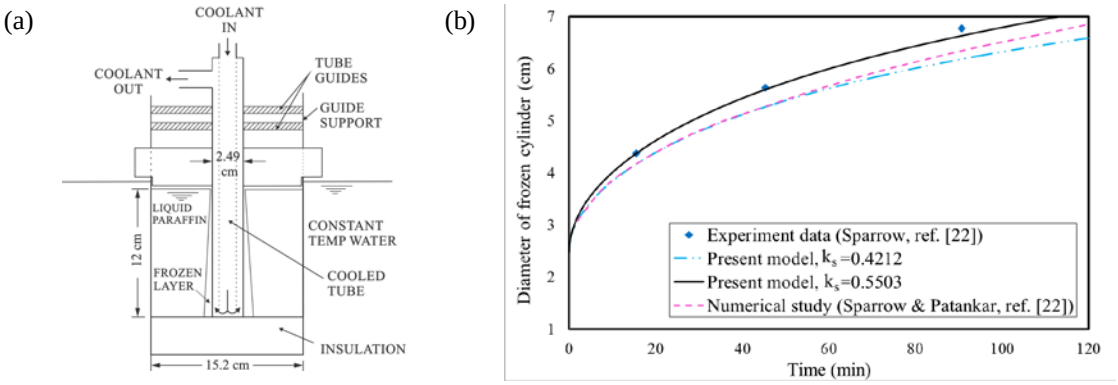

Fig. 3. (a) Experimental apparatus [22], and (b) Position of solid-liquid interface versus time for freezing in a non-superheated liquid

Case III. Melting in anannularTES during charging process

The results of melting in an annular TES system, simulated usingthis model,arecompared with the results from steady-state asymptote. An annular pipe similar to the geometry shown in Fig.1, with constant temperature at both walls is studied.Figure4 (a) shows the moving boundary location as a function of time for different Stefan numbers. The aspect ratio, ε, is equal to 0.5 and the difference between the dimensionless temperatures of the inner and outer walls is3. Other dimensionless parameters are:k^*=0.8, α^*=0.5, and q^*_{gen}=0. For allStefan numbers, the melting front starts from the inner pipe, ε=0.5, and the location of interface at equilibrium state is independent of the Stefan number. The steady-state location obtained from the present lumped parameter model is 0.7671, in good agreement with the steady-state exact solution, i.e., 0.7660.The slope of this graph (Fig. 4a), which represents the velocity of the interface, is related to the Stefan number. As the Stefan number increases, the melting process reaches the steady state condition faster.The dimensionless heat flux at the inner and outer

wall is shown in Fig. 4 (b).Again, the model results are in good agreement with the steady state exact solutions. The dimensionless heat flux at the outer pipe obtained from the present lumped parameter model is -6.1694while thevalue from the exact solution is -6.0593. The same agreement was achieved for the dimensionless heat flux at the inner wall: 12.3408 forlumped parameter model and 12.1186 from the exact solution. Thus, the results from the steady state region of the present model are validated with exact solutions and maximum relative difference of 1.8% has been observed.

Having dimensionless heat fluxes at both walls, the rate of stored energy can be evaluated for a confined PCM by writing the energy balance, $E_{stored}=\delta E_{in}-\delta E_{out}=\delta E/_{r=a}-\delta E/_{r=b}$. The dimensionless rate of stored energy is derived as follows

$$\frac{\dot{E}_{stored}}{\dot{E}_{ref}} = \varepsilon k^{*}\left(\partial\theta_{l}/\partial\xi\right)\Big|_{\xi=\varepsilon} - \left(\partial\theta_{s}/\partial\xi\right)\Big|_{\xi=1} \tag{16}$$

Figure4(c) shows the changes of dimensionless rate of stored energy over dimensionless time during melting, charging process. At small Fourier numbers, there is a rise in stored energy because of the rapid growth of the melted region in PCM, which then settles to zero, the steady state condition. The area below this curve represents the total energy stored in the PCM, which can be obtained by integrating the rate of stored energy over time. Charging is complete when the rate of energy storage reacheszero. The energy storage density (ESD) is defined as stored energy divided by volume of PCM, and is derived indimensionless form in equation (17). Fig. 4(d) shows the dimensionless energy storage density through the time. At each time*Fo*, ESD can be obtained from this graph. Considering the whole charging process, dimensionless ESD is equal to 1.2634.

$$\frac{ESD}{ESD_{ref}} = \frac{\left(\varepsilon k^{*}\left(\partial\theta_{l}/\partial\xi\right)\big|_{\xi=\varepsilon} - \left(\partial\theta_{s}/\partial\xi\right)\big|_{\xi=1}\right)Fo}{1-\varepsilon^{2}} \tag{17}$$

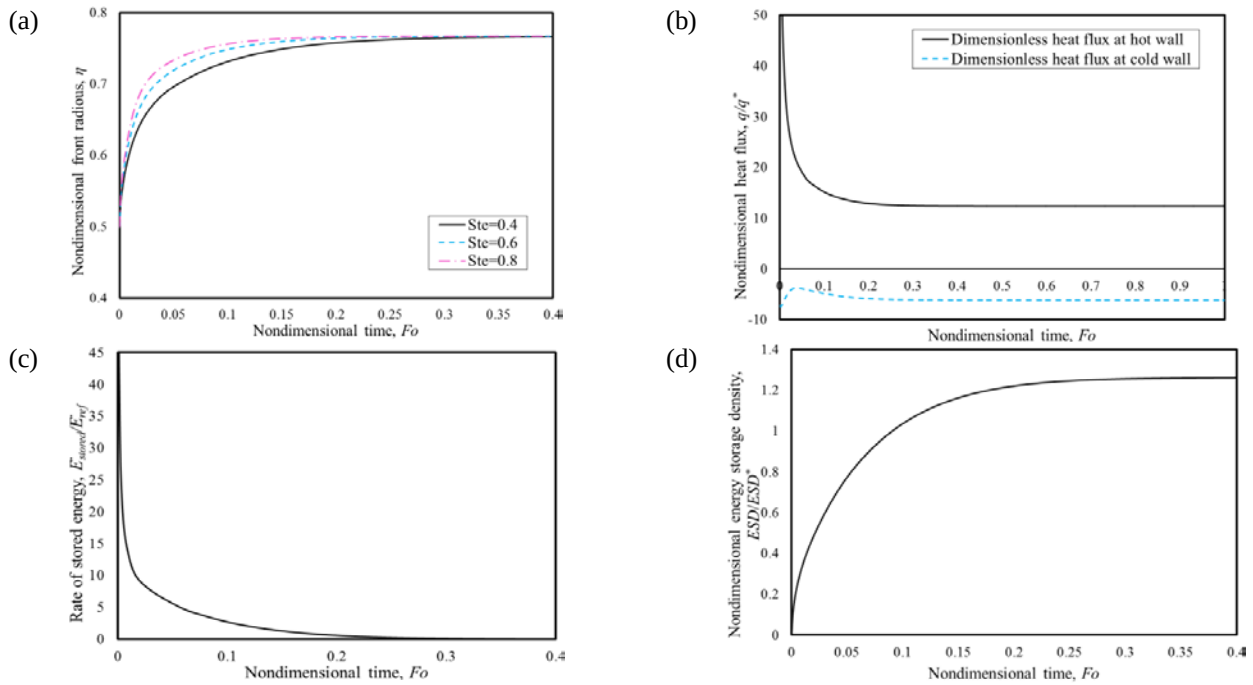

Fig. 4. (a) Dimensionless interface location over dimensionless time with different Stefan numbers,(b) dimensionless heat flux predicted by the present model at the inner and outer walls, (c) dimensionless rate of stored energy, and (d) dimensionless energy storage density during the charging process

CONCLUSIONS

The melting process wasanalyzed with an improved lumped parameter model using Hermite two-point approximation for averaged temperatures and heat fluxes. The model showedgood agreementwith exact solutions of the short- and long-term asymptotes for solidification due to a line heat sink in the center of a cylindrical pipe, as well as existing experimental data for solidification in annular pipes having constant temperatures at walls. Moreover, as a case study, melting in annular TESwasstudied.The effect of Stefan number, which is a key parameter in TES, on the location of the interface at equilibrium was found to be independent of the Stefan number, and as the Stefan number increases the melting process reaches the steady state condition much faster.Important parameters in assessing TES systems, the stored energy and charging/discharging timewere studied in the present modelstored energy can beobtained bythe dimensionless heat fluxes at inner and outer walls. The proposed model is applicable for a variety of boundary conditions such as constant temperature, adiabatic, constant heat flux and convective conditions.Moreover, thepresent easy-to-use model can be utilized to find storage efficiency and energy storage density to perform optimized design of latent TES systems.

Acknowledgments

Special thanks to Dr. Claire McCague and Dr. Wendell Huttema.The authors gratefully acknowledge the financial support of the Natural Sciences and Engineering Research Council of Canada (NSERC) through Automotive Partnership Canada Grant No. APCPJ 401826-10.

Nomenclature

c_p	specific heat, ($J/(kgK)$)	t	time (s)
$E_{ref}^{\cdot}$	reference rate of energy, $E_{ref}^{\cdot} = 2\pi k_s l\,(T_m-T_b)$	Greek letters	
ESD_{ref}	dimensionless energy storage density, $ESD_{ref} = k_s\,(T_m-T_b)$	α	thermal diffusivity (m^2/s)
		α^*	dimensionless thermal diffusivity, $\alpha^*=\alpha_l / \alpha_s$
Fo	thermal Fourier number, $Fo=\alpha_s t/r_b^2$	ε	aspect ratio of inner pipe to outer pipe, $\varepsilon=r_a / r_b$
H	Hermite approximation	η	dimensionless location of solid-liquid interface, $\eta(Fo)=S(t) / r_b$
k	thermal conductivity ($W/(mK)$)		
k^*	dimensionless thermal conductivity, $k^*=k_l / k_s$	θ	dimensionless temperature, $\theta=(T(r,t)-T_b) /(T_m-T_b)$
L	latent heat of melting (J/kg)	ξ	dimensionless space coordinate, $\xi=r/r_b$
l	length of the annular pipes (m)	ρ	similarity parameter
$q^{\cdot}$	volumetric heat generation (W/m^3)	λ	similarity parameter
q^{*}_{gen}	dimensionless volumetric heat generation, $q^{*}_{gen}=r^2_{ref} q^{\cdot}_{gen}/(k_s(T_m-T_b))$	Subscripts	
		a	inner wall ($\xi=\varepsilon$)
$q^{''}_{ref}$	reference heat flux, $q^{''}_{ref} =k_s(T_m-T_b)/r_b$	b	outer wall ($\xi=1$)
Q^*	dimensionless heat sink strength, $Q^*=Q/(2\pi k_s(T_m-T_b))$	i	initial
		l	liquid
r	radial coordinate (m)	ref	reference
Ste	Stefan number, $Ste=c_{p,s}\,(T_m-T_b)/L$	s	solid
S	location of interface (m)	Superscripts	
T	temperature (K)	$\bar{}$	averaged value between $\xi=\varepsilon$ and $\xi=1$
T_m	melting temperature (K)	$*$	dimensionless value

References

1. ItenM., LiuS. A work procedure of utilizing PCMs as thermal storage systems based on air-TES systems // *Energy Conversion and Management*. 2014. Vol. 77 Pp. 608-627.
2. Carslaw H. S., Conard Jaeger J.*Conduction of heat in solids*, Oxford University Press, New York, 1959.
3. Özisik M. N.*Heat Conduction*, Wiley-Interscience, New York,1993.
4. Paterson S. Propagation of a Boundary of Fusion // *Proceedings of the Glasgow Mathematical Association.*1939. Vol. 1. Pp. 42-47.

5. Cho C., Özisik M.N. Effect of radiation on melting of semi-infinite medium //*Proc. 6th Heat Transfer Conf.*, 1978, Pp. 373–378.
6. Cao Y., and Faghri A. Performance characteristics of a thermal energy storage module: a transient PCM/forced convection conjugate analysis //*International Journal of Heat and Mass Transfer*, 1991. Vol. 34(1). Pp. 93–101.
7. Dalhuijsen A.J., Segal A. Comparison of finite element techniques for conduction problems //*Int J Numer Meth Eng*. 1986. Vol. 23. Pp. 1807–29.
8. Yohei Y., Bojan N. A sharp-interface phase change model for a mass-conservative interface tracking method // *Journal of Computational Physics.* 2013. Vol. 249 Pp.127-161.
9. Rongzong H., Wu H., Cheng P. A new lattice Boltzmann model for solid–liquid phase change //*International Journal of Heat and Mass Transfer*. 2013. Vol. 59. Pp. 295-301.
10. Voller V.R. Fast implicit finite-difference method for the analysis of phase change problems // *Numer Heat Transfer Part.* 1990 Vol. 17. Pp. 155–69.
11. Goodman T. R. The heat-balance integral and its application to problems involving a change of phase //*Trans. ASME*. 1958. Vol. 80 (2). Pp. 335–342.
12. Mitchell S.L., Myers T. G. Improving the accuracy of heat balance integral methods applied to thermal problems with time dependent boundary conditions //*International Journal of Heat and Mass Transfer.*2010. Vol. 53(17). Pp. 3540-3551.
13. Sadoun N., Si-AhmedE-K. A new analytical expression for the freezing constant in the Stefan problem with initial superheating // *Numerical methods in thermal problems.* 1995. Vol. 9. Pp. 843-854.
14. Mitchell S.L., Myers T.G. Application of Heat Balance Integral Methods to one-dimensional phase change problems //*International Journal of Differential Equations.* 2012.Vol. 2012. Pp. 1-22.
15. Jiji L. M., Gaye S. Analysis of solidification and melting of PCM with energy generation // *Appl. Therm. Eng*. 2006. Vol. 26 (5-6). Pp. 568-575.
16. Mirzaei P. A., Haghighat F. Modeling of phase change materials for applications in whole building simulation //*Renew. Sustain. Energy Rev.* 2012. Vol. 16(7). Pp. 5355–5362.
17. Cotta R. M., Mikhailov M. D. *Heat Conduction: Lumped Analysis, Integral Transforms, Symbolic Computation*, Wiley-Interscience, 1997.
18. An C., Su J. Lumped parameter model for one-dimensional melting in a slab with volumetric heat generation //*Applied Thermal Engineering*. 2013. Vol. 60. Pp. 387-396.
19. Regis C. R., Cotta R. M., Su J. Improved lumped analysis of transient heat conduction in a nuclear fuel rod //*Int. Commun. Heat Mass Transfer*. 2000. Vol. 27. Pp. 357-366.
20. Su J. Improved lumped models for transient radioactive cooling of a spherical body // *Int. Commun. Heat Mass Transfer*. 2004. Vol. 31. Pp. 85-94.
21. Mennig J., Auerbach T., Hälg W. Two point Hermite approximations for the solution of linear initial value and boundary value problems //*Comput. Method. Appl. Mech*. 1983. Vol. 39 (2). Pp.199-224.
22. Sparrow E. M., RamseyJ. W., KeminkR. G., Freezing controlled by natural convection // *J. Heat Transfer*. 1979. Vol. 101(4). Pp. 578-584.
23. StrykerP.C., SparrowE.M. Application of a spherical thermal conductivity cell to solid n-eicosane paraffin // *Int. J. Heat Mass Transfer*.1990. Vol. 33.Pp. 1781–1793.
24. NabilM., KhodadadiJ.M. Experimental determination of temperature-dependent thermal conductivity of solid eicosane-based nanostructure-enhanced phase change materials // *International Journal of Heat and Mass Transfer.*2013. Vol. 67. Pp. 301–310.
25. IsmailK. A. R., GonçalvesM. M. Thermal performance of a PCM storage unit // *Energy Conversion & Management*. 1999. Vol. 40. Pp. 115-138